

## New Superconducting and Semiconducting Fe-B Compounds Predicted with an *Ab Initio* Evolutionary Search

A. N. Kolmogorov,<sup>1</sup> S. Shah,<sup>1</sup> E. R. Margine,<sup>1</sup> A. F. Bialon,<sup>2</sup> T. Hammerschmidt,<sup>2</sup> and R. Drautz<sup>2</sup>

<sup>1</sup>*Department of Materials, University of Oxford, Parks Road, Oxford OX1 3PH, United Kingdom*

<sup>2</sup>*Atomistic Modelling and Simulation, ICAMS, Ruhr-Universität Bochum, D-44801 Bochum, Germany*

(Received 20 April 2010; published 19 November 2010)

New candidate ground states at 1:4, 1:2, and 1:1 compositions are identified in the well-known Fe-B system via a combination of *ab initio* high-throughput and evolutionary searches. We show that the proposed *oP12*-FeB<sub>2</sub> stabilizes by a break up of 2D boron layers into 1D chains while *oP10*-FeB<sub>4</sub> stabilizes by a distortion of a 3D boron network. The uniqueness of these configurations gives rise to a set of remarkable properties: *oP12*-FeB<sub>2</sub> is expected to be the first semiconducting metal diboride and *oP10*-FeB<sub>4</sub> is shown to have the potential for phonon-mediated superconductivity with a  $T_c$  of 15–20 K.

DOI: 10.1103/PhysRevLett.105.217003

PACS numbers: 74.70.Ad, 31.15.A–, 61.66.Dk, 62.20.–x

A range of advanced compound prediction methods has been developed recently to accelerate the experimental search for materials displaying novel physics or technologically relevant features [1–4]. Unconstrained structural optimization with evolutionary algorithms (EAs) has shown the ability to predict complex configurations given only the composition leading to identification of exotic high-pressure phases [3]. High-throughput screening with data mining techniques has proven effective in revealing compositions favorable to form in large sets of multicomponent systems [4]. In this study we demonstrate that new ambient-pressure materials with appealing properties could be found in such a well-known and accessible binary system as Fe-B.

The experimental research on Fe-B compounds has been driven primarily by their potential to serve as a hardening agent in steels [5] or as hard protective coatings [6,7]. According to the latest experimental phase diagram [8], FeB and Fe<sub>2</sub>B are the only reproducible low temperature phases that have been shown to crystallize in the *oP8* (or the related *oS8* [9]) and *tI12* configurations, respectively. Less is known about the boron-rich ordered phases with only a few reports available: observation of a metastable FeB<sub>49</sub> intercalation compound [10] and possible synthesis of amorphous [11] and the AlB<sub>2</sub>-type [12] iron diborides. Previous modelling work on Fe-B compounds has given insights into their binding, magnetic, and structural properties [13–18] but has not systematically explored the possibility of obtaining new stable iron borides.

Our reexamination of the Fe-B system within density functional theory (DFT) begins with a high-throughput scan of known configurations listed in the Inorganic Crystal Structure Database ICSD [19]. We show that never observed *oP6*-FeB<sub>2</sub> (*hP6*-FeB<sub>2</sub>) and *tI16*-FeB phases are marginally stable relative to the known compounds. The proposed Fe-B ground states are then refined with an *ab initio* evolutionary search that suggests *oP10*-FeB<sub>4</sub> and *oP12*-FeB<sub>2</sub> to be ground states at 1:4 and 1:2 compositions.

The prediction of the brand new stable structure types is surprising as transition metal (TM) borides tend to crystallize in configurations correlating well between the 3*d*, 4*d*, and 5*d* series [20]. We link the stabilization of the Fe-B phases to the structural changes in the B networks that lead to radically new properties. At 1:2 metal-boron composition, famous for the outstanding MgB<sub>2</sub> superconductor [21] and the hardest metal-based ReB<sub>2</sub> material [22], *oP12*-FeB<sub>2</sub> stands out as the first semiconducting metal diboride made out of B chains rather than B layers. At 1:4 composition, the nonmagnetic *oP10*-FeB<sub>4</sub> is examined using electron-phonon (*e-ph*) calculations and predicted to be, subject to spin fluctuation effects [23], a superconductor with an unexpectedly high  $T_c$  of 15–20 K. The critical temperature falls between the typical 10 K  $T_c$  of TM borides [24] and the 39 K  $T_c$  of MgB<sub>2</sub> [21]. If synthesized, *oP10*-FeB<sub>4</sub> could extend the family of recently discovered iron-based LaFeAsO<sub>1-x</sub>F<sub>x</sub> and FeSe superconducting materials [25] but have the conventional phonon-mediated coupling mechanism.

We carry out the high-throughput scan by calculating formation enthalpies at  $T = 0$  K and  $P = 0$  GPa with VASP [26] for over 40 commonly observed *M-B* and *M-C* ICSD structure types [27] in the whole composition range. The B-rich end of the phase diagram is further explored with the Module for *Ab Initio* Structure Evolution (MAISE) [28] linked with VASP which enables an EA search for the lowest enthalpy ordered phases. The unconstrained structural optimization is carried out for most likely to occur 1:6, 1:4, 1:3, and 1:2 compositions starting from random unit cells of up to 15 atoms (for further details see supplementary material [27]).

Finding ground states also depends on the accuracy of the simulation method and the inclusion of important Gibbs energy contributions [1]. We use the projector augmented waves method [29] and allow spin polarization unless stated otherwise; the chosen energy cutoff of 500 eV and dense Monkhorst-Pack  $k$  meshes [30] ensure

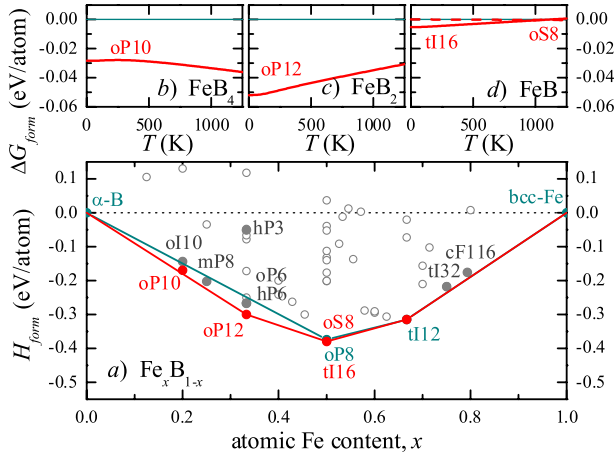


FIG. 1 (color online). Stability of Fe-B alloys calculated with GGA-PBE: (a) formation enthalpy; (b)–(d) Gibbs energy with thermodynamic corrections due to the vibrational entropy for selected candidate phases with respect to the  $\alpha$ -B  $\leftrightarrow$   $oP8$ -FeB tieline.

numerical convergence of formation energy differences to typically 1–2 meV/atom. We employ the Perdew-Burke-Ernzerhof (PBE) exchange-correlation ( $xc$ ) functional [31] within the generalized gradient approximation (GGA) that provides a realistic description of the Fe ground state [32]. Tests in the supplementary material [27] demonstrate independence of our key finding, the stability of new phases at the 1:2 and 1:4 Fe-B compositions with respect to known compounds, on the choice of the  $xc$  functional. The ground state of B is modeled as  $\alpha$ -B which has been recently shown to be only 3–4 meV/atom above the more complex  $\beta$ -B in the 0–300 K temperature range [33]. We include phonon corrections to  $G(T)$  using a finite displacement method as implemented in PHON [34]. The  $e$ -ph calculations are carried out within the linear response theory using the QUANTUM-ESPRESSO package [35,36]. Our tests show no magnetic moment in relevant B-rich phases allowing us to do the EA, phonon, and  $e$ -ph simulations without spin polarization.

Figure 1(a) summarizes calculated  $T = 0$  K formation energies of the considered  $\text{Fe}_x\text{B}_{1-x}$  ordered structures with the convex hull drawn (in cyan) through the known  $oP8$ -FeB and  $tI12$ -Fe<sub>2</sub>B ground states; other relevant  $oI10$ ,  $oP10$ ,  $mP8$ ,  $hP3$ ,  $hP6$ ,  $oP6$ ,  $oP12$ ,  $oS8$ ,  $tI16$ ,  $tI32$  and  $cF116$  structures correspond to the  $\text{CrB}_4$ ,  $\text{FeB}_4$  (proposed),  $\text{FeB}_3$  (proposed),  $\text{AlB}_2$ ,  $\text{ReB}_2$ ,  $\text{RuB}_2$ ,  $\text{FeB}_2$  (proposed),  $\text{CrB}$ ,  $\text{MoB}$ ,  $\text{Ni}_3\text{P}$ , and  $\text{Cr}_{23}\text{C}_6$  prototypes, respectively. Phases with  $x > 0.5$  show an expected ordering, with  $tI12$ -Fe<sub>2</sub>B being stable and  $\text{Fe}_3\text{B}$  and  $\text{Fe}_{23}\text{B}_6$  being metastable by less than 20 meV/atom. For  $x \leq 0.5$ , we find a set of phases that are below or close to the  $\alpha$ -B  $\leftrightarrow$   $oP8$ -FeB tieline to be viable ground state candidates. We discuss their relative stability using structural and electronic density of states (DOS) information shown in Figs. 2 and 3.

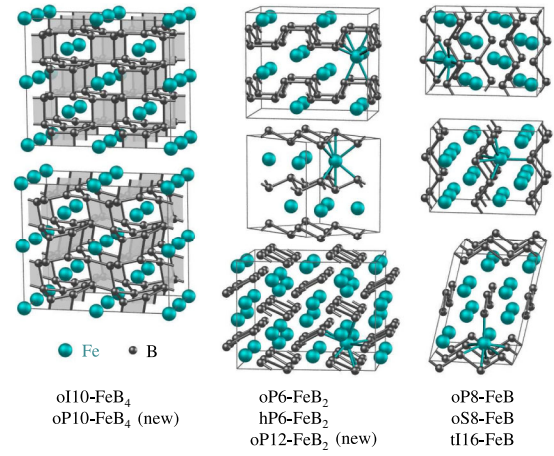


FIG. 2 (color online). Competing B-rich Fe-B phases; cell parameters are given in the supplementary material [27].

The similarity of the local coordinations in  $oP8$ ,  $oS8$ , and  $tI16$  at 1:1 composition was discussed previously in Ref. [37]. In  $tI16$  the B chains extend in two directions, a feature that could differentiate the structure's mechanical response to external load from the behavior of the other two polymorphs. Figure 1(d) reflects the difference in the vibrational properties of  $oP8$  ( $oS8$ ) and  $tI16$  and could explain why  $tI16$ -FeB, marginally the most stable phase at  $T = 0$  K in our calculations, has never been observed. The electronic DOS of FeB in the three configurations are rather similar (Fig. 3): they are all metallic and magnetic and have bonding  $p$ - $d$  hybridized states in the  $-6$ – $-3$  eV energy range.

At 1:2 composition, all known metal borides stable under normal conditions are composed of 2D boron layers that are flat in  $hP3$ , armchair in  $oP6$ , zigzag in  $hP6$ , or mixed in  $hR18$  [19]. A detailed rigid band approximation study of the  $\text{TMB}_2$  phases linked the distortion of the B layers to population of antibonding TM-TM and TM-B orbitals in  $hP3$ - $\text{TMB}_2$  with high  $d$ -electron count [13]. The projected DOS in  $hP3$ -FeB<sub>2</sub> (Fig. 3) shows a mismatch in the maxima of the filled B and Fe states in the  $-7$ – $-3$  eV range and a high DOS at the Fermi level resulting in a magnetic moment of  $0.26\mu_B$ /atom. The magnetization energy of 11 meV/atom is insufficient to stabilize the  $hP3$ -FeB phase which leaves it 200 meV/atom above the  $\alpha$ -B  $\leftrightarrow$   $oP8$ -FeB tieline. Puckering of the B layers in nonmagnetic  $oP6$  and  $hP6$  proves to be a more favorable way of reducing the high DOS at the Fermi level: Fig. 3 shows a higher hybridization of the B- $p$  and Fe- $d$  states with the antibonding  $p$ - $d$  states now lying just above  $E_F$ . The net result of the more bimodal shape of the DOS is a 217 meV/atom gain in stability. Even more dramatic structural and electronic changes take place in  $oP12$ -FeB<sub>2</sub> discovered in our EA search. The disintegration of the B layers opens up a  $\sim 0.5$  eV band gap (likely underestimated in our semilocal DFT treatment [38]) and leads to an additional 33 meV/atom gain in stability. This finding rules out the existence of  $hP3$ -FeB<sub>2</sub> that has been a

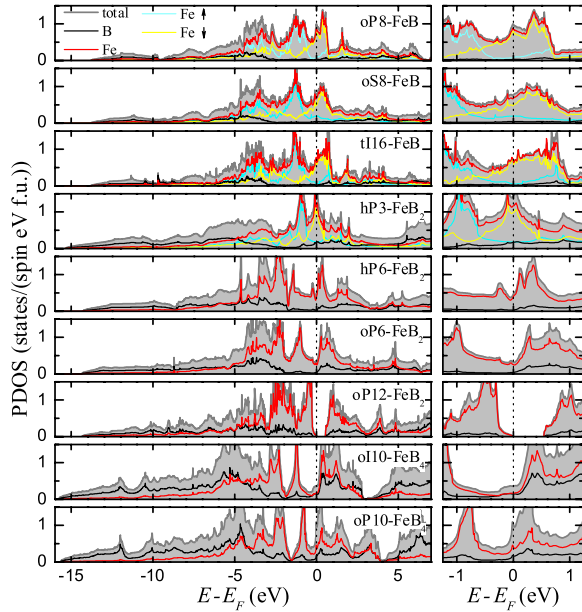


FIG. 3 (color online). Calculated density of states in selected iron borides (the lower five compounds are nonmagnetic).

subject of controversy [39];  $oP12\text{-FeB}_2$  is below the  $\alpha\text{-B} \leftrightarrow oP8\text{-FeB}$  tieline by over 30 meV/atom [Fig. 1(c)] in the whole  $T$  range and should be synthesizable.

At 1:3 composition, the EA suggests a new  $mP8$  phase [27] that breaks the  $\alpha\text{-B} \leftrightarrow oP8\text{-FeB}$  tieline by 15 meV/atom; however it is found to be metastable with respect to  $\alpha\text{-B}$  and  $oP12\text{-FeB}_2$  at all temperatures.

At 1:4 composition, the observed proximity of the  $oI10\text{-FeB}_4$  phase to the  $\alpha\text{-B} \leftrightarrow oP8\text{-FeB}$  tieline is intriguing as there have been explicit references to unsuccessful attempts to synthesize this phase [14]. Unexpectedly, a phonon dispersion calculation showed dynamical instability of  $oI10\text{-FeB}_4$ , with imaginary frequencies reaching  $208i\text{ cm}^{-1}$  for a  $\Gamma$ -point phonon in the conventional 10-atom unit cell. Using the phonon eigenvector that skews the rectangle B building units in the  $x$ - $y$  plane into parallelograms we have constructed a new structure type,  $oP10\text{-FeB}_4$ . The considerable energy gain of 28 meV/atom and no imaginary frequencies in the phonon spectrum make  $oP10\text{-FeB}_4$  thermodynamically and dynamically stable in the considered temperature range relative to known phases [Fig. 1(b)]; with phonon corrections included  $oP10\text{-FeB}_4$  lies 3 meV/atom above the  $\alpha\text{-B} \leftrightarrow oP12\text{-FeB}_2$  tieline at  $T = 0\text{ K}$  but 10 meV/atom below the tieline at  $T = 900\text{ K}$ . Additional no-symmetry relaxations of distorted  $oI10$  and  $oP10$  supercells with 10, 20, and 40 atoms have consistently produced  $oP10\text{-FeB}_4$  as the most stable configuration. The EA search has also shown that  $\text{Fe}_2\text{B}_8$  cells converge to  $oP10\text{-FeB}_4$  while  $\text{Fe}_3\text{B}_{12}$  cells evolve into a new  $mS30\text{-FeB}_4$  phase metastable by 6 meV/atom. The tests seemed necessary due to a counter-intuitive evolution of the DOS in the  $oI10$  to  $oP10$  transformation: the Fermi level in  $oP10\text{-FeB}_4$  catches the edge

of the antibonding  $p_{x,y} - d_{x^2-y^2}$  peak resulting in a high  $n(E_F) = 1.0$  states/(eV spin f.u.); the feature is unusual as stable compounds tend to have the Fermi level lying in the pseudogap [40].

The naturally electron-doped  $oP10\text{-FeB}_4$  candidate material with strong covalent bonds is next analyzed for superconducting features. We use the linear response theory and fine  $k$  and  $q$  meshes [27,36] to calculate the phonon DOS (PHDOS), Eliashberg function ( $\alpha^2 F(\omega)$ ), and strength of the  $e$ -ph coupling ( $\lambda(\omega)$ ). The phonon spectrum in Fig. 4 can be divided into three regions with mixed Fe-B modes ( $0\text{--}320\text{ cm}^{-1}$ ), B modes with a relatively flat PHDOS ( $320\text{--}740\text{ cm}^{-1}$ ), and B modes involving in-plane optical distortions of B parallelograms ( $860\text{--}920\text{ cm}^{-1}$ ). The Eliashberg function integrates to a large  $\lambda_{\text{tot}} = 0.80$  and gives the logarithmic average  $\langle\omega\rangle_{\text{ln}} = 430\text{ cm}^{-1}$ . While key contributions to  $\lambda_{\text{tot}} \sim 0.8$  in  $\text{CaB}_6$  and  $\text{MgB}_2$  come from the low-frequency Ca modes ( $\omega < 150\text{ cm}^{-1}$ ) [41] and the high-frequency B modes ( $500\text{ cm}^{-1} < \omega < 560\text{ cm}^{-1}$ ) [42], respectively, nearly 60% of  $\lambda_{\text{tot}}$  in  $oP10\text{-FeB}_4$  is generated by the mixed Fe-B modes in the  $160\text{--}300\text{ cm}^{-1}$  range.  $\langle\omega\rangle_{\text{ln}}$  in  $oP10\text{-FeB}_4$  is found to be much closer to the  $\text{MgB}_2$  value of  $\sim 450\text{ cm}^{-1}$  [42], rather than the  $\text{CaB}_6$  value of  $\sim 200\text{ cm}^{-1}$  [41]. Using the Allen-Dynes formula [43] and typical  $\mu^*$  of 0.14–0.10 we estimate the  $T_c$  in  $oP10\text{-FeB}_4$  to be 15–20 K. The compound has two 3D Fermi surfaces centered at  $\Gamma$  and  $R$  points and the  $T_c$  may be further enhanced by the multiband effect. Because of the large gradient of the DOS near the Fermi level the superconducting properties may be strongly affected by the presence of vacancies or impurities. Although  $oP10\text{-FeB}_4$  is found to have neither ferro- nor antiferromagnetic moment, spin fluctuations [23] could play a critical role in the pairing mechanism and should be examined carefully using input from experiment.

In summary, our search for new compounds in the common Fe-B system demonstrates the necessity to go beyond standard structure types: The EA-driven unconstrained

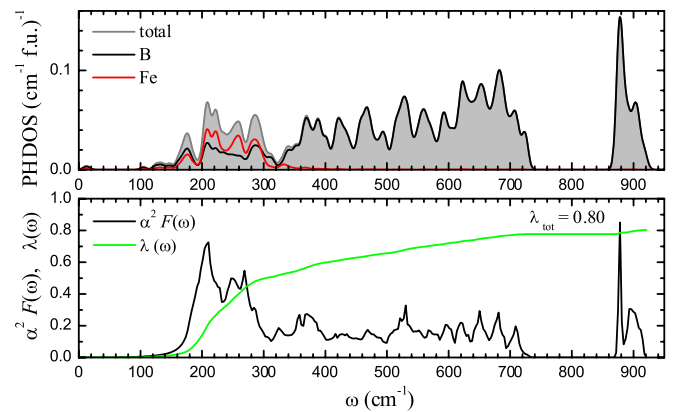


FIG. 4 (color online). Top: total and projected phonon density of states (PHDOS) in  $oP10\text{-FeB}_4$ . Bottom: Eliashberg function and the strength of the electron-phonon coupling.

structural optimization has uncovered a set of viable ground states, with new *oP10*-FeB<sub>4</sub> and *oP12*-FeB<sub>2</sub> shown to be thermodynamically stable by over 25 meV/atom relative to the known  $\alpha$ -B and *oP8*-FeB. To the best of our knowledge, the identified boron-rich phases have been never observed before and their discovery may require finding suitable kinetic routes. The presented analysis of the structural and electronic properties shows how the phases stabilize and what new physics they are expected to exhibit if synthesized. (i) *oP10*-FeB<sub>4</sub> could become yet another exception to Matthias' rules [44] that recommend staying away from magnetic elements when designing new superconductors. This compound has a high DOS at the Fermi level leading to  $\lambda_{\text{tot}} = 0.80$  and a surprisingly high  $T_c$  of 15–20 K. (ii) *oP12*-FeB<sub>2</sub> is predicted to be the first metal diboride semiconductor with a  $\sim 0.5$  eV band gap (time-dependent DFT or Green's functions techniques will likely give a larger value [38]). (iii) The proposed materials may also exhibit appealing mechanical properties as hardness tends to be higher for  $M_xB_{1-x}$  with  $x < 0.5$  [22].

A. N. K. and S. S. acknowledge the support of the EPSRC and the Oxford Supercomputing Centre. A. F. B., T. H., and R. D. acknowledge financial support through ThyssenKrupp AG, Bayer MaterialScience AG, Salzgitter Mannesmann Forschung GmbH, Robert Bosch GmbH, Benteler Stahl/Rohr GmbH, Bayer Technology Services GmbH and the state of North-Rhine Westphalia as well as the EU in the framework of the ERDF.

- 
- [1] S. W. Woodley and R. Catlow, *Nature Mater.* **7**, 937 (2008).
- [2] R. Martoňák, A. Laio, and M. Parrinello, *Phys. Rev. Lett.* **90**, 075503 (2003); S. Curtarolo *et al.*, *Phys. Rev. Lett.* **91**, 135503 (2003); C. C. Fischer *et al.*, *Nature Mater.* **5**, 641 (2006); G. Trimarchi, A. J. Freeman, and A. Zunger, *Phys. Rev. B* **80**, 092101 (2009); C. J. Pickard and R. J. Needs, *Phys. Rev. Lett.* **97**, 045504 (2006).
- [3] A. R. Oganov and C. W. Glass, *J. Phys. Condens. Matter* **20**, 064210 (2008); A. R. Oganov *et al.*, *Nature (London)* **457**, 863 (2009).
- [4] G. Hautier *et al.*, *Chem. Mater.* **22**, 3762 (2010).
- [5] L. Lanier, G. Metauer, and M. Moukassi, *Mikrochim. Acta* **114–115**, 353 (1994); S. Watanabe, H. Ohtani, and T. Kunitake, *Trans. ISIJ* **23**, 120 (1983).
- [6] I. Campos *et al.*, *Mater. Sci. Eng. A* **352**, 261 (2003).
- [7] S. Sen, U. Sen, and C. Bindal, *Vacuum* **77**, 195 (2005).
- [8] T. van Rompaey, K. C. Hari Kumar, and P. Wollants, *J. Alloys Compd.* **334**, 173 (2002).
- [9] V. A. Barinov *et al.*, *Phys. Status Solidi A* **123**, 527 (1991); T. Kanaizuka, *Phys. Status Solidi A* **69**, 739 (1982).
- [10] K. Balani, A. Agarwala, and N. B. Dahotre, *J. Appl. Phys.* **99**, 044904 (2006).
- [11] K. Moorjani *et al.*, *J. Appl. Phys.* **57**, 3444 (1985).
- [12] L. G. Voroshnin *et al.*, *Met. Sci. Heat Treat. [Metal. i Term. Obrabotka Metal.]* **12**, 732 (1970).
- [13] J. K. Burdett, E. Canadell, and G. J. Miller, *J. Am. Chem. Soc.* **108**, 6561 (1986).
- [14] J. K. Burdett and E. Canadell, *Inorg. Chem.* **27**, 4437 (1988).
- [15] P. Mohn and D. G. Pettifor, *J. Phys. C* **21**, 2829 (1988).
- [16] P. Mohn, *J. Phys. C* **21**, 2841 (1988).
- [17] W. Y. Ching *et al.*, *Phys. Rev. B* **42**, 4460 (1990).
- [18] P. R. Ohodnicki, Jr. *et al.*, *Phys. Rev. B* **78**, 144414 (2008).
- [19] G. Bergerhoff and I. D. Brown, in *Crystallographic Databases*, edited by F. H. Allen *et al.* (International Union of Crystallography, Chester, 1987).
- [20] J. J. Zuckerman and A. P. Hagen, *Inorganic Reactions and Methods: Formation of Bonds to Group-I, -II, and -IIIB Elements*, Vol. 13 (Wiley, New York, 2007), Chap. 6.7.
- [21] J. Nagamatsu *et al.*, *Nature (London)* **410**, 63 (2001).
- [22] H.-Y. Chung *et al.*, *Science* **316**, 436 (2007).
- [23] I. I. Mazin *et al.*, *Phys. Rev. Lett.* **101**, 057003 (2008); M. Wierzbowska, *Eur. Phys. J. B* **48**, 207 (2005); S. K. Bose *J. Phys. Condens. Matter* **21**, 025602 (2009).
- [24] J. W. Simonson *et al.*, *J. Supercond. Novel Magnetism* **23**, 417 (2010) and references therein.
- [25] Y. Kamihara *et al.*, *J. Am. Chem. Soc.* **130**, 3296 (2008); F. C. Hsu *et al.*, *Proc. Natl. Acad. Sci. U.S.A.* **105**, 14262 (2008); I. I. Mazin, *Nature (London)* **464**, 183 (2010).
- [26] G. Kresse and J. Hafner, *Phys. Rev. B* **47**, 558 (1993); G. Kresse and J. Furthmüller, *Phys. Rev. B* **54**, 11169 (1996).
- [27] See supplementary material at <http://link.aps.org/supplemental/10.1103/PhysRevLett.105.217003>.
- [28] A. N. Kolmogorov, <http://maise-guide.org>.
- [29] P. E. Blöchl, *Phys. Rev. B* **50**, 17953 (1994).
- [30] J. D. Pack and H. J. Monkhorst, *Phys. Rev. B* **13**, 5188 (1976); **16**, 1748 (1977).
- [31] J. P. Perdew, K. Burke, and M. Ernzerhof, *Phys. Rev. Lett.* **77**, 3865 (1996).
- [32] L. Vočadlo *et al.*, *Faraday Discuss.* **106**, 205 (1997).
- [33] M. J. van Setten *et al.*, *J. Am. Chem. Soc.* **129**, 2458 (2007).
- [34] D. Alfé, *Comput. Phys. Commun.* **180**, 2622 (2009).
- [35] P. Giannozzi *et al.*, <http://www.quantum-espresso.org>.
- [36] We employ ultrasoft pseudopotentials [D. Vanderbilt, *Phys. Rev. B* **41**, R7892 (1990)] with a cutoff of 43 and 344 Ry for the wave functions and charge density, respectively. A  $9 \times 9 \times 18$  *k*-point mesh with a Gaussian smearing of 0.02 Ry and a  $3 \times 3 \times 6$  *q* mesh are used for phonon dispersion calculations; a  $18 \times 18 \times 36$  *k* mesh is used to evaluate the *e*-ph coupling.
- [37] D. Hohnke and E. Parthé, *Acta Crystallogr.* **20**, 572 (1966).
- [38] G. Onida, L. Reining, and A. Rubio, *Rev. Mod. Phys.* **74**, 601 (2002).
- [39] L. Topor and O. J. Kleppa, *J. Chem. Thermodyn.* **17**, 1003 (1985); A. F. Guillermet and G. Grimvall, *J. Less-Common Met.* **169**, 257 (1991).
- [40] A. N. Kolmogorov and S. Curtarolo, *Phys. Rev. B* **74**, 224507 (2006) and references therein.
- [41] M. Calandra and F. Mauri, *Phys. Rev. Lett.* **95**, 237002 (2005).
- [42] A. Y. Liu, I. I. Mazin, and J. Kortus, *Phys. Rev. Lett.* **87**, 087005 (2001).
- [43] P. B. Allen and R. C. Dynes, *Phys. Rev. B* **12**, 905 (1975).
- [44] W. E. Pickett, *Physica (Amsterdam)* **296B**, 112 (2001).